ice cover causes high attenuation as frequency increases, limiting long-range propagation to very low frequencies. Bathymetric effects are important near the major ocean ridges, basin margins, and on the shelf areas where significant mode coupling can occur. The Arctic sound channel is very stable and predictable in the central Arctic basins and there is a close correspondence of propagating acoustic modes with the major water masses of the Arctic Ocean, especially the important AIW. This latter fact makes the use of acoustic thermometry for monitoring long-term Arctic Ocean temperature change particularly suitable. Ongoing research is exploring ways to relate changes in acoustic travel time and intensity to monitor other important variables in the Arctic Ocean including changes in the PW, DW, and the halocline, and average sea-ice thickness and roughness. The latter measurements, when combined with sea ice extent from satellite remote sensing, could provide an estimate of sea ice mass in the Arctic (*see* **Satellite Passive Microwave Measurements of Sea Ice**).

The role of the Arctic Ocean in shaping and responding to global climate change is only beginning to be explored. Cost-effective, long-term, year-round synoptic observations in the Arctic Ocean require new measurement strategies. The year-round ice cover in the Arctic prevents the use of satellites for direct ocean observations common in the ice-free oceans. Shore-cabled mooring-based observations using advanced biogeochemical sensors and acoustic sources and hydrophone arrays, as well as instrumented autonomous underwater vehicles (AUVs) and under-ice drifters, represent new approaches for observing the Arctic Ocean (*see* **Autonomous Underwater Vehicles (AUVs)**). Interestingly the RAFOS concept (using nonexplosive sources) is being evaluated anew as a way to track AUVs and drifters in the Arctic as well as for acoustic communication of data. It is clear that Arctic acoustics will have as large a role to play in this important new endeavor in the future, as it has had in the submarine and military operations of the past.

See also

Acoustics, Arctic. Acoustics in Marine Sediments. Acoustic Noise. Acoustics, Shallow Water. Arctic Basin Circulation. Autonomous Underwater Vehicles (AUVs). Bioacoustics. Ice–Ocean Interaction. Nepheloid Layers. North Atlantic Oscillation (NAO). Satellite Passive Microwave Measurements of Sea Ice. Sea Ice: Overview; Variations in Extent and Thickness. Seals. Seismic Structure. Thermohaline Circulation. Tomography. Under-ice Boundary Layer. Water Types and Water Masses.

Further Reading

Dyer I (1984) Song of sea ice and other Arctic Ocean melodies. In: Dyer I and Chryssostomidis C (eds) *Arctic Technology and Policy*, 11–37. Washington, DC: Hemisphere Publishing.

Dyer I (1993) Source mechanisms of Arctic Ocean ambient noise. In: Kerman BR (ed.), *Natural Physical Sources of Underwater Sound*, 537–551. Netherlands: Kluwer Academic.

Leary WM (1999) *Under Ice*. College Station: Texas A&M University Press.

LePage K and Schmidt H (1994) Modeling of low-frequency transmission loss in the central Arctic. *Journal of the Acoustic Society of America* 96(3): 1783–1795.

Mikhalevsky PN, Gavrilov AN and Baggeroer AB (1999) The transarctic acoustic propagation experiment and climate monitoring in the Arctic. *IEEE Journal of Oceanic Engineering* 24(2): 183–201.

Newton JL (1989) Sound speed structure of the Arctic Ocean including some effects on acoustic propagation. *US Navy Journal of Underwater Acoustics* 39(4): 363–384.

Richardson WJ, Greene CR Jr, Malme CI and Thomson DH (1995) *Marine Mammals and Noise*. San Diego: Academic Press.

Urick RJ (1975) *Principles of Underwater Sound*. New York: McGraw-Hill.

Von Winkle WA (ed.) (1984) *Naval Underwater Systems Center (NUSC) Scientific and Engineering Studies: Underwater Acoustics in the Arctic*. New London: Naval Underwater Systems Center Publisher.

ACOUSTICS, DEEP OCEAN

W. A. Kuperman, Scripps Institution of Oceanography, University of California, San Diego, CA, USA

Copyright © 2001 Academic Press

doi:10.1006/rwos.2001.0312

Introduction

The acoustic properties of the ocean, such as the paths along which sound from a localized source will travel, are mainly dependent on its sound speed structure. The sound speed structure is dependent

on the oceanographic environment described by variations in temperature, salinity, and density with depth or horizontal position. This article will review the ocean acoustic environment, sound propagation, ambient noise, scattering and reverberation, and the passive and active sonar equation.

Ocean Acoustic Environment

Sound propagation in the ocean is governed by the spatial structure of the sound speed and the sound speed in the ocean is a function of temperature, salinity, and ambient pressure. Since the ambient pressure is a function of depth, it is customary to express the sound speed (c) in meters per second as an empirical function of temperature (T) in degrees celsius, salinity (S) in parts per thousand and depth (z) in meters, e.g. eqn [1].

$$c = 1449.2 + 4.6T - 0.055T^2 + 0.00029T^3 + (1.34 - 0.01T)(S - 35) + 0.016z \qquad [1]$$

There exist more accurate formulas, if needed.

Figure 1 shows a typical set of sound speed profiles, indicating greatest variability near the surface. In a warmer season (or warmer part of the day, sometimes referred to as the 'afternoon effect'), the temperature increases near the surface and hence the sound speed increases toward the sea surface. In nonpolar regions where mixing near the surface due to wind and wave activity is important, a mixed layer of almost constant temperature is often created. In this isothermal layer, sound speed increases with depth because of the increasing ambient pressure, the last term in eqn [1]. This is the surface duct region. Below the mixed layer is the thermocline where the temperature and hence the sound speed decrease with depth. Below the thermocline, the temperature is constant and the sound speed increases because of increasing ambient pressure. Therefore, between the deep isothermal region and the mixed layer, there is a minimum sound speed; the depth at which this minimum takes place is referred to as the axis of the deep sound channel. However, in polar regions, the water is coldest near the surface so that the minimum sound speed is at the surface.

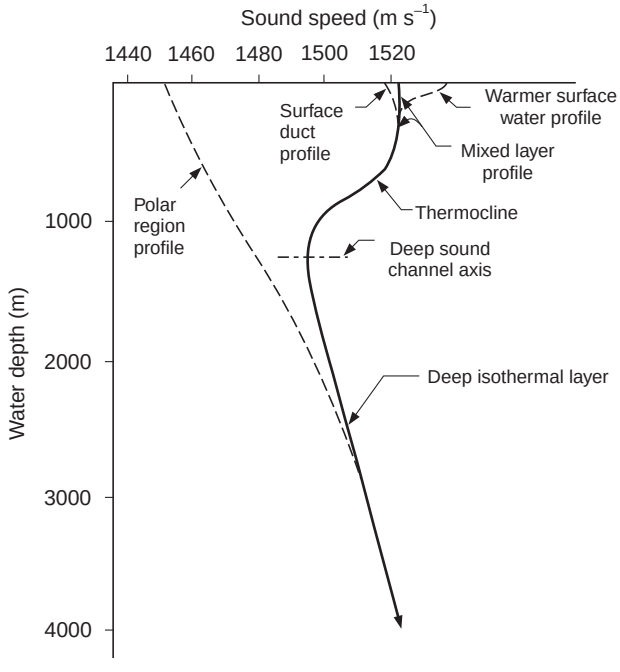

Figure 1 Generic sounds speed profiles.

Figure 2 is a contour display of the sound speed structure of the North and South Atlantic with the deep sound channel axis indicated by the heavy dashed line. Note that the deep sound channel becomes shallower toward the poles. Aside from sound speed effects, the ocean volume is absorbtive and will cause attenuation that increases with acoustic frequency.

The ocean surface and bottom also have a strong influence on sound propagation. The ocean surface, though a perfect reflector when flat, causes scattering when its roughness becomes comparable in size with the acoustic wavelength. The ocean bottom, depending on its local structure will scatter and also attenuate the acoustic field.

Units

The decibel (dB) denotes a ratio of intensities (see Section 3.3) expressed in terms of a logarithmic (base 10) scale. The ratio of two intensities, I_1/I_2 is $10\log(I_1/I_2)$ in dB units. Absolute intensities are expressed using an accepted reference intensity of a plane wave having an rms pressure equal to 10^{-5} dyn cm^{-2} or, equivalently, 1 μPa. Transmission loss is a decibel measure of relative intensity, the latter being proportional to the square of the acoustic amplitude.

Sound Propagation

Very Short-range Propagation

The pressure amplitude from a point source in free space falls off with range r as r^{-1}; this geometric loss is called spherical spreading. Most sources of interest in the deep ocean are nearer the surface than the bottom. Hence, the two main short-range

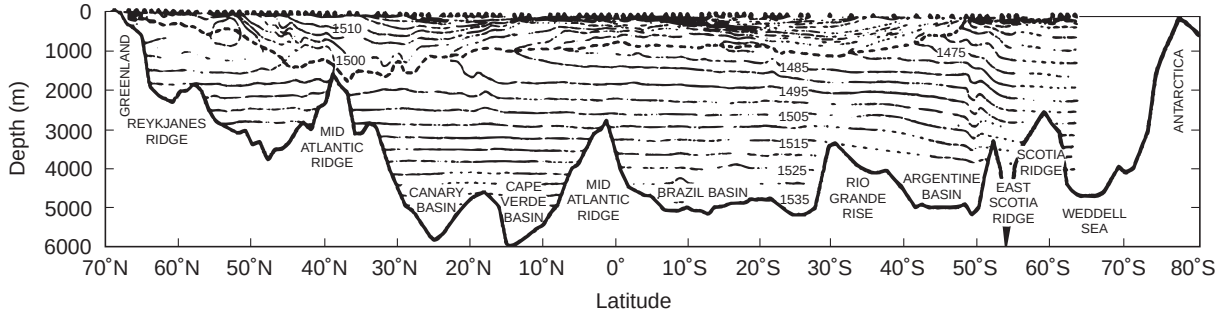

Figure 2 Sound speed contours of the North and South Atlantic along 30.50°W. Dashed line indicates axis of deep sound channel. (From Northrop and Colborn (1974).)

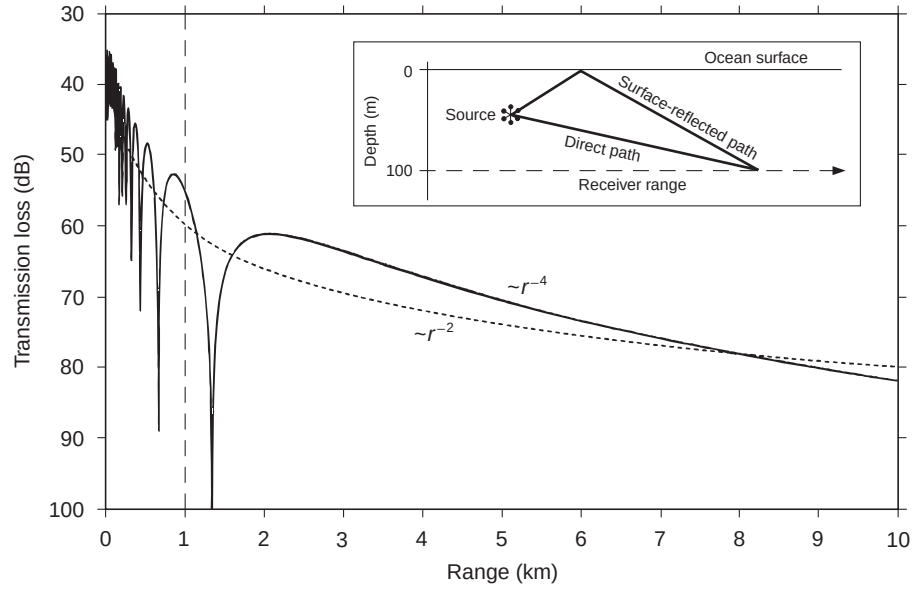

Figure 3 The insert shows the geometry of the Lloyd mirror effect. The plots show a comparison of Lloyd mirror to spherical spreading. Transmission losses are plotted in decibels corresponding to losses of $10 \log r^2$ and $10 \log r^4$, respectively, as explained in the test.

paths are the direct path and the surface-reflected path. When these two paths interfere, they produce a spatial distribution of sound often referred to as a 'Lloyd mirror pattern' as shown in the insert of **Figure 3**.

Basic Long-range Propagation Paths

Figure 4 is a schematic of propagation paths in the ocean resulting from the sound speed profiles (indicated by the dashed line) described above in **Figure 1**. These paths can be understood from Snell's law eqn [2], which relates the ray angle $\theta(z)$, with respect to the horizontal, to the local sound speed $c(z)$ at depth z.

$$\frac{\cos \theta(z)}{c(z)} = \text{constant} \qquad [2]$$

The equation requires that the higher the sound speed, the smaller the angle with the horizontal, meaning that sound bends away from regions of high sound speed or, put another way, sound bends toward regions of low sound speed. Therefore, paths A, B, and C are the simplest to explain since they are paths that oscillate about the local sound speed minima. For example, path C depicted by a ray leaving a source near the deep sound channel axis at a small horizontal angle propagates in the deep sound channel. This path, in temperate latitudes where the sound speed minimum is far from the surface, permits propagation over distances of thousands of kilometers. Path D, which is at slightly steeper angles and is usually excited by a near surface source, is convergence zone propagation, a spatially periodic (35–65 km) refocusing phenomenon producing zones of high intensity near

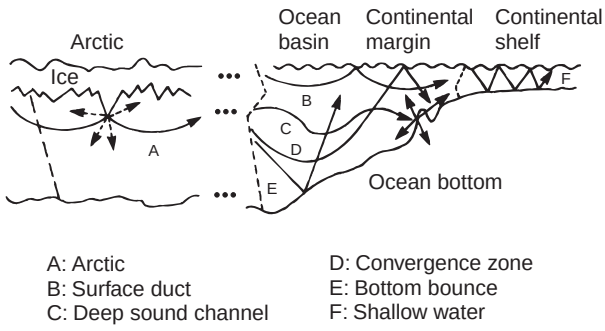

Figure 4 Schematic representation of sound propagations paths in the ocean.

the surface due to the upward refracting nature of the deep sound speed profile. Regions between these zones are referred to as shadow regions. Referring back to **Figure 1**, there may be a depth in the deep isothermal layer at which the sound speed is the same as it is at the surface; this depth is called the critical depth and is the lower limit of the deep sound channel. A positive critical depth specifies that the environment supports long-distance propagation without bottom interaction, whereas a negative critical depth specifies that the ocean bottom is the lower boundary of the deep sound channel. The bottom bounce path E is also a periodic phenomenon but with a shorter cycle distance and shorter propagation distance because of losses when sound is reflected from the ocean bottom.

An alternative way of describing paths is by denoting that they are composed of combinations of refraction (R), surface reflection (SR) and bottom reflection (BR) processes. Thus, **Figure 4** also represents some of these paths. Note from Snell's law that refractive paths involve a path turning around at the highest speed in its duct of confinement. Because such ray paths spend much of their propagation in regions of high sound speed, larger launch angle paths with longer path lengths arrive earlier than shorter paths launched at shallower angles. This is just the opposite of boundary-limited propagation such a bottom bounce (or shallow water) in which a reflection occurs before refraction in a high-speed region can take place. Hence, for deep water refractive paths, those paths that penetrate to a deeper depth have a greater group speed (the horizontal speed of energy propagation) than those paths that do not go as deep, with the axial, most horizontal path along the deep sound channel axis having the slowest group speed. For pulse propagation, this axial arrival is the last arrival.

Geometric Spreading Loss

The energy per unit time emitted by a sound source flows through a larger area with increasing range. Intensity is the power flux through a unit area, which translates to the energy flow per unit time through a unit area. Hence, the simplest example of geometric loss is spherical spreading for a point source in free space, for which the area increases as $4\pi r^2$, where r is the range from the point source. Thus spherical spreading results in an intensity decay proportional to r^{-2}. Since intensity is proportional to the square of the pressure amplitude, the fluctuations in pressure p induced by the sound decay as r^{-1}. For range-independent ducted propagation, that is, where rays are refracted or reflected back toward the horizontal direction (which is the case for most long-range propagation), there is no loss associated with the vertical dimension. In this case, the spreading surface is the area of a cylinder whose axis is in the vertical direction passing through the source: $2\pi rH$ where H is the depth of the duct and is constant. Geometric loss in the near-field Lloyd mirror regime requires consideration of interfering beams from direct and surface reflected paths. To summarize, the geometric spreading laws for the pressure field (recall that intensity is proportional to the square of the pressure) are

- Spherical spreading loss: $p \propto r^{-1}$
- Cylindrical spreading loss: $p \propto r^{-1/2}$
- Lloyd mirror loss: $p \propto r^{-2}$.

Volume Attenuation

Volume attenuation increases with frequency. In **Figure 3**, the losses associated with path C include only volume attenuation and scattering because this path does not involve boundary interactions. The volume scattering can be biological in origin or can arise from interaction with large internal wave activity in the vicinity of the upper part of the deep sound channel where paths are refracted before they would interact with the surface. Both of these effects are small for low frequencies. This same internal wave region is also on the lower boundary of the surface duct, allowing scattering out of the surface duct and thereby also constituting a loss mechanism for the surface duct. This mechanism also leaks sound into the deep sound channel, a region that without scattering would be a shadow zone for a surface duct source. This type of scattering from internal waves is also thought to be a major source of fluctuation of the sound field.

Attenuation is characterized by an exponential decay of the sound field. If A_0 is the rms amplitude

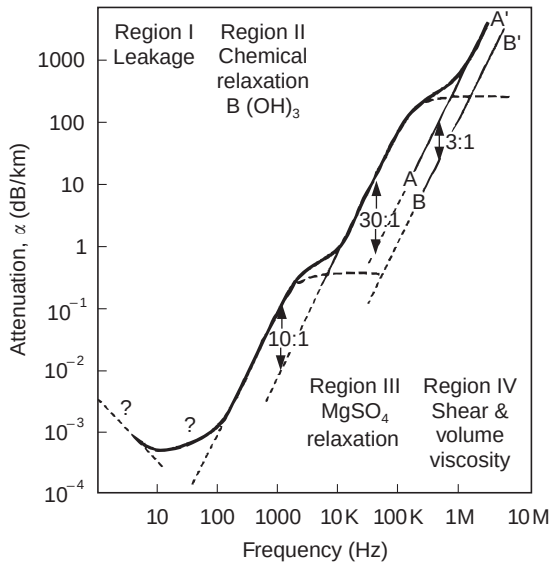

Figure 5 Regions of different dominant processes of attenuation of sound in sea water. (From Urick (1979).) The attenuation α is given in dB per 1000 yards.

of the sound field at unit distance from the source, then the attenuation of the sound field causes the amplitude to decay with distance r along the path according to eqn [3], where the unit of α is nepers/distance (nepers is a unitless quantity).

$$A = A_0 \exp(-\alpha r), \qquad [3]$$

This attenuation coefficient can be expressed in decibels per unit distance by the conversion $\alpha' = 8.686\alpha$. The frequency dependence of attenuation can be roughly divided into four regimes as displayed in **Figure 5**. In region I, leakage out of the sound channel is believed to be the main cause of attenuation. The main mechanisms associated with regions II and III are boric acid and magnesium sulfate chemical relaxation. Region IV is dominated by the shear and bulk viscosity associated with fresh water. A summary of the approximate frequency dependence (f in kHz) of attenuation (in units of dB km^{-1}) is given in eqn [4] with the terms sequentially associated with regions I–IV in **Figure 5**.

$$\alpha'(dB\,km^{-1}) = 3.3 \times 10^{-3} + \frac{0.11f^2}{1+f^2} + \frac{43f^2}{4100+f^2} + 2.98 \times 10^{-4} f^2 \qquad [4]$$

Bottom Loss

The structure of the ocean bottom affects those acoustic paths that interact with the ocean bottom. This bottom interaction is summarized by bottom

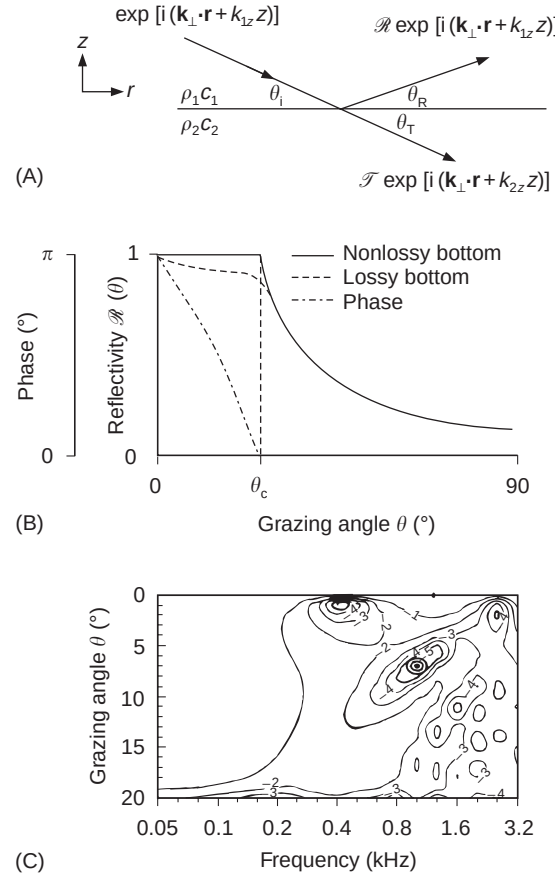

Figure 6 The reflection and transmission processes. Grazing angles are defined relative to the horizontal. (A) A plane wave is incident on an interface separating two media with densities and sound speeds ρ, c. $\mathscr{R}(\theta)$ and $\mathscr{T}(\theta)$ are reflection and transmission coefficients. Snell's law is a statement that $k_\perp$, the horizontal component of the wavevector, is the same for all three waves. (B) Rayleigh reflection curve (eqn [5]) as a function of the grazing angle (θ in (A)) indicating critical θ_c. The dashed curve shows that if the second medium is lossy, there is less than perfect reflection below the critical angle. (C) Examples of contour of reflection loss ($20 \log \mathscr{R}$) for a layered bottom, showing frequency and grazing angle dependence. The simpler reflectivity curve for each frequency is obtained from a vertical slice.

reflectivity, the amplitude ratio of reflected and incident plane waves at the ocean-bottom interface as a function of grazing angle, θ (see **Figure 6A**). For a simple bottom that can be represented by a semi-infinite half-space with constant sound speed c_b and density ρ_b, the reflectivity is given by eqn [5] with the subscript w denoting water

$$\mathscr{R}(\theta) = \frac{\rho_b k_{wz} - \rho_w k_{bz}}{\rho_b k_{wz} + \rho_w k_{bz}}, \qquad [5]$$

The wavenumbers are given by eqn [6].

$$k_{iz} = (\omega/c_i)\sin\theta_i = k \sin\theta_i; \qquad i = w, b \qquad [6]$$

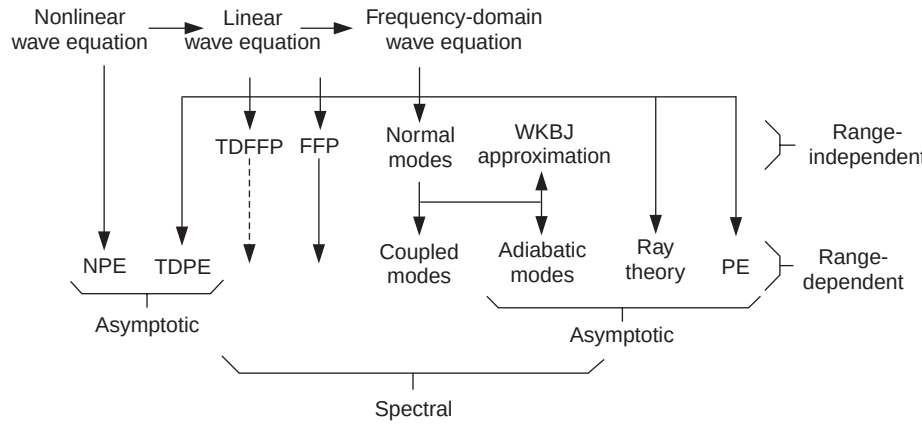

Figure 7 Heirarchy of underwater acoustic models. TD refers to time domain. NPE is the nonlinear parabolic equation that describes high-amplitude (e.g., shockwave) propagation. The arrows are directed toward the flow of derivation of the model.

The incident and transmitted grazing angles are related by Snell's law according to eqn [7] and the incident grazing angle θ_w is also equal to the angle of the reflected plane wave.

$$c_b \cos\theta_w = c_w \cos\theta_b \qquad [7]$$

For this simple water-bottom interface for which we take $c_b > c_w$, there exists a critical grazing angle θ_c below which there is perfect reflection (eqn [8]).

$$\cos\theta_c = \frac{c_w}{c_b} \qquad [8]$$

For a lossy bottom, there is no perfect reflection, as also indicated in a typical reflection curve in **Figure 6B**. These results are approximately frequency independent. However, for a layered bottom, the reflectivity has a complicated frequency dependence as shown in the example in **Figure 6C**, where the contours are in decibels. This example shows the simple reflectivity result below 200 Hz and then a more complicated frequency dependence at higher frequencies. It should be pointed out that if the density of the second medium vanishes, the reflectivity reduces to the pressure release case of $\mathscr{R}(\theta) = -1$.

Propagation Models

An ocean acoustic environment is often very complex, with range- and depth-dependent properties. Such an environment does not in general lend itself to simple analytic predictions of sound propagation. Even in range-independent environments there are many paths (multipaths) and these paths combine to form a complex interference pattern. For example, the convergence zones are an example of a more complex structure that cannot be described by a monotonic geometric spreading law. Acoustic models play an important role in predicting sound propagation; the inputs to these models are oceanographic quantities ultimately translated into the acoustically relevant parameters of sound speed, density, and attenuation.

Sound propagation in the ocean is mathematically described by the wave equation whose coefficients and boundary conditions are derived from the ocean environment. There are essentially four types of models (computer solutions to the wave equation) to describe sound propagation in the sea: ray, spectral or fast field program (FFP), normal mode (NM), and the parabolic equation (PE). Ray theory is an asymptotic high-frequency approximation to the wave equation, whereas the latter three models are more or less direct solutions to the wave equations under an assortment of milder restrictions. The high-frequency limit does not include diffraction phenomena. All of these models can handle depth variation of the ocean acoustic environment. A model that also takes into account horizontal variations in the environment (i.e., sloping bottom or spatially variable oceanography) is termed range-dependent. For high frequencies (a few kHz or above), ray theory is the most practical. The other three model types are more applicable and usable at lower frequencies (below 1 kHz). The hierarchy of underwater acoustic models is shown in schematic form in **Figure 7**. The output of these models is typically propagation loss, which is the intensity relative to a unit source at unit distance, expressed in decibels. Transmission loss is the negative of propagation loss, and hence, a positive quantity.

An example of the output of propagation models is shown in **Figure 8**, indicating agreement between the models. However, we also see a difference

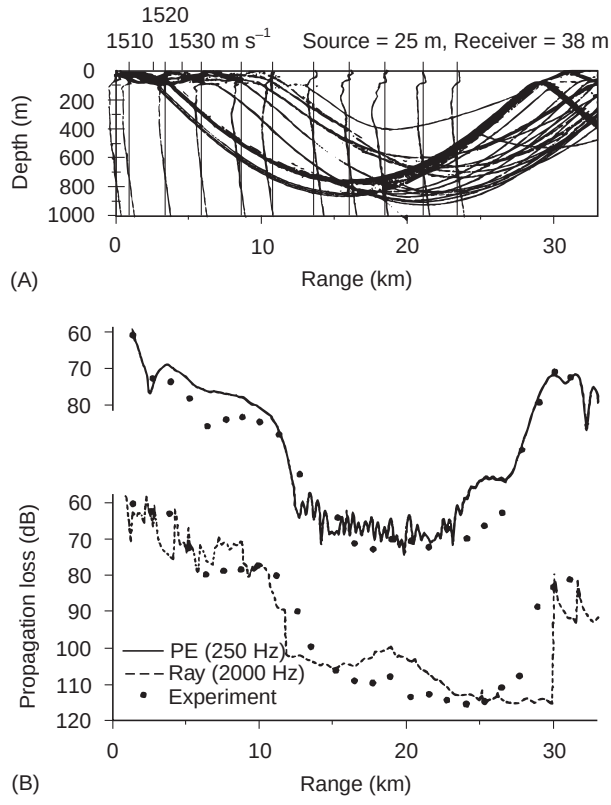

Figure 8 Model and data comparison for a range-dependent deep water case. (A) Sound speed profiles as a function of range together with a ray trace showing the breakdown of surface duct propagation. (B) Parabolic equation comparison with data at 250 Hz and ray theory comparison with data at 2000 Hz.

among the models in that ray theory predicts a sharper shadow zone than the wave theory model (i.e., the 10–30 km region in **Figure 8B**); this is an expected result from the infinite-frequency ray approximation.

Scattering and Reverberation

Scattering caused by rough boundaries or volume inhomogeneities is a mechanism for loss (attenuation), reverberant interference, and fluctuation. Attenuation from volume scattering was addressed above. In most cases, it is the mean or coherent (or specular) part of the acoustic field that is of interest for a sonar or communications application, and scattering causes part of the acoustic field to be randomized. Rough surface scattering out of the 'specular direction' can be thought of as an attenuation of the mean acoustic field and typically increases with increasing frequency. A formula often used to describe reflectivity from a rough boundary is eqn [9], where $\mathscr{R}(\theta)$ is the reflection coefficient of the smooth interface and Γ is the Rayleigh roughness parameter defined as $\Gamma \equiv 2k\sigma \sin\theta$ where $k = 2\pi/\lambda, \lambda$ is the acoustic wavelength, and σ is the rms roughness (height).

$$\mathscr{R}'(\theta) = \mathscr{R}(\theta)\exp -\frac{\Gamma^2}{2} \qquad [9]$$

The scattered field is often referred to as reverberation. Surface, bottom, or volume scattering strength, $S_{S,B,V}$ is a simple parametrization of the production of reverberation and is defined as the ratio in decibels of the sound scattered by a unit surface area or volume referenced to a unit distance, I_{scat}, to the incident plane wave intensity, I_{inc} (eqn [10]).

$$S_{S,B,V} = 10\log\frac{I_{scat}}{I_{inc}} \qquad [10]$$

The Chapman–Harris curves predicts the ocean surface scattering strength in the 400–6400 Hz region; eqn [11], where θ is the grazing angle in degrees, w the wind speed in $m\,s^{-1}$ and f is the frequency in Hz.

$$S_S = 3.3\,\beta\log\frac{\theta}{30} - 42.4\log\beta + 2.6;$$

$$\beta = 107(wf^{1/3})^{-0.58} \qquad [11]$$

A more elaborate formula exists that is more accurate for lower wind speeds and lower frequencies.

The simple characterization of bottom backscattering strength utilizes Lambert's rule for diffuse scattering, given by eqn [12] where the first term is determined empirically.

$$S_B = A + 10\log\sin^2\theta \qquad [12]$$

Under the assumption that all incident energy is scattered into the water column with no transmission in to the bottom, A is -5 dB. Typical realistic values for A that have been measured are -17 dB for big Basalt Mid-Atlantic Ridge cliffs and -27 dB for sediment ponds.

Volume scattering strength is typically reduced to a surface scattering strength by taking S_V as an average volume scattering strength within some layer at a particular depth; then the corresponding surface scattering strength is given by eqn [13], where H is the layer thickness.

$$S_S = S_V + 10\log H \qquad [13]$$

The column or integrated scattering strength is defined as the case for which H is the total water depth.

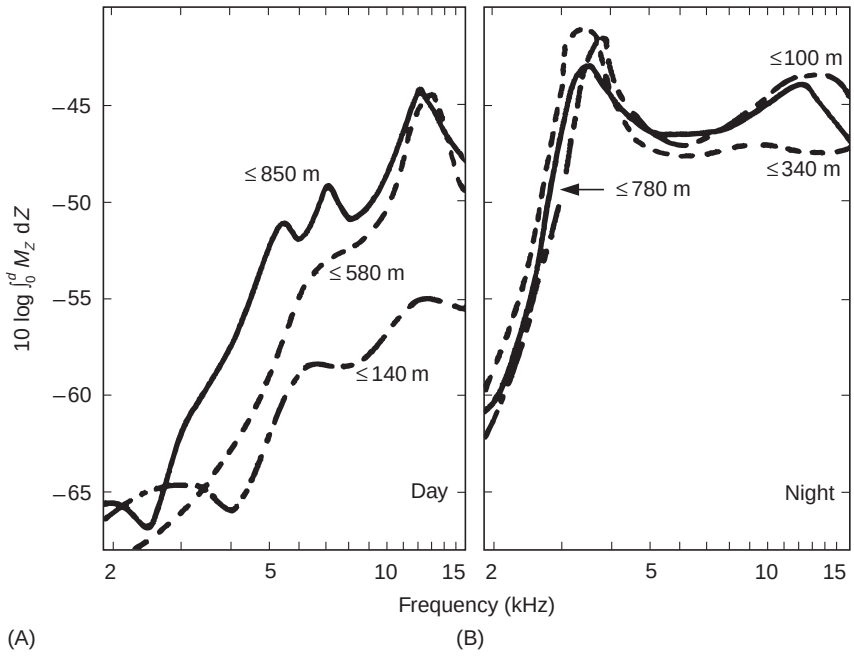

Figure 9 Day and night scattering strength measurements using an explosive source as a function of frequency. The spectra measured at various times after the explosion are labeled with the depth of the nearest scatterer that could have contributed to the reverberation. The ordinate corresponds to S_v in eqn [13]. (From Chapman and Marchall (1966).)

Volume scattering usually decreases with depth (about 5 dB per 300 m) with the exception of the deep scattering layer. For frequencies less than 10 kHz, fish with air-filled swimbladders are the main scatterers. Above 20 kHz, zooplankton or smaller animals that feed upon phytoplankton and the associated biological chain are the scatterers. The deep scattering layer (DSL) is deeper in the day than in the night, changing most rapidly during sunset and sunrise. This layer produces a strong scattering increase of 5–15 dB within 100 m of the surface at night and virtually no scattering in the daytime at the surface since it migrates down to hundreds of meters. Since higher pressure compresses the fish swimbladder, the backscattering acoustic resonance tend to be at a higher frequency during the day when the DSL migrates to greater depths. Examples of day and night scattering strengths are shown in **Figure 9**.

Finally, near-surface bubbles and bubble clouds can be thought of as either volume or surface scattering mechanisms acting in concert with the rough surface. Bubbles have resonances (typically greater than 10 kHz) and at these resonances, scattering is strongly enhanced. Bubble clouds have collective properties; among these properties is that a bubbly mixture, as specified by its void fraction (total bubble gas volume divided by water volume) has a considerable lower sound speed than water.

Ambient Noise

There are essentially two types of ocean acoustic noise: man-made and natural. Generally, shipping is the most important source of man-made noise, though noise from offshore oil rigs is becoming more and more prevalent. Typically, natural noise dominates at low frequencies (below 10 Hz) and high frequencies (above a few hundred hertz). Shipping fills in the region between ten and a few hundred hertz. A summary of the spectrum of noise is shown in **Figure 10**. The higher-frequency noise is usually parametrized according to sea state (also Beaufort number) and/or wind. **Table 1** summarizes the description of sea state.

The sound speed profile affects the vertical and angular distribution of noise in the deep ocean. When there is a positive critical depth, sound from surface sources can travel long distances without interacting with the ocean bottom, but a receiver below this critical depth should sense less surface noise because propagation involves interaction with lossy boundaries, surface and/or bottom. This is illustrated in **Figure 11**, which shows a deep water environment with measured ambient noise. **Figure 12** is an example of vertical directivity of noise that also follows the propagation physics discussed above. The shallower depth is at the axis of the deep sound channel, while the other is at the critical

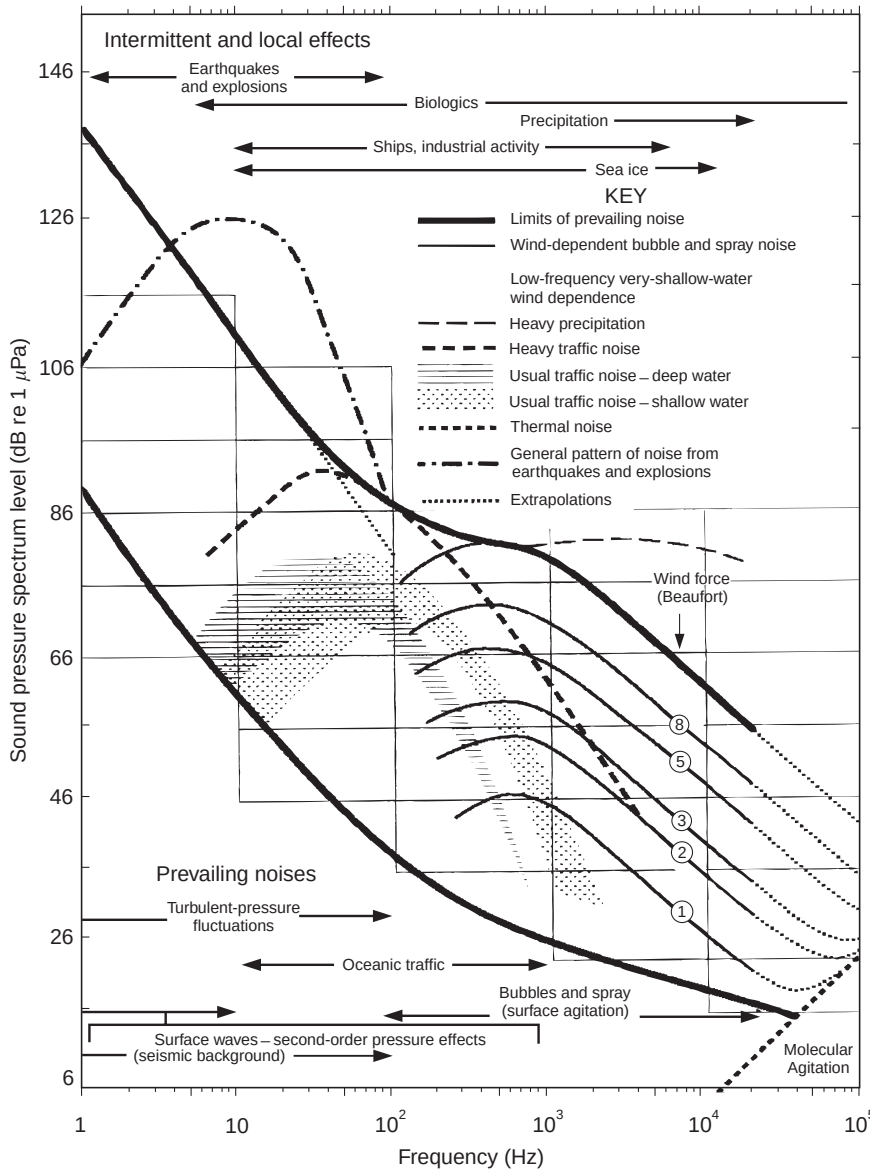

Figure 10 Composite of ambient noise spectra. (From Wenz (1962).)

depth. The pattern is narrower at the critical depth where the sound paths tend to be horizontal since the rays are turning around at the lower boundary of the deep sound channel.

In a range-independent ocean, Snell's law predicts a horizontal noise notch at depths where the speed of sound is less than the near-surface sound speed. Returning to eqn [2] and reading off the sound speeds from **Figure 11** at the surface ($c = 1530\,\mathrm{m\,s^{-1}}$) and say, 300 m ($1500\,\mathrm{m\,s^{-1}}$), a horizontal ray ($\theta = 0$) launched from ocean surface would have an angle with respect to the horizontal of about 11° at 300 m depth. All other rays would arrive with greater vertical angles. Hence we expect this horizontal notch. However, the horizontal notch is often not seen at shipping noise frequencies. This is because shipping tends to be concentrated in continental shelf regions; range-dependent propagation couples such noise sources to the deep ocean. Thus, for example, propagation down a continental slope converts high-angle rays to lower angles at each bounce. There are also deep sound channel shoaling effects that result in the same trend in angle conversion.

Sonar Equation

A major application of underwater acoustics is sonar technology. The performance of a sonar is often described simply in terms of the sonar

Table 1 Descriptions of the ocean sea surface. Approximate relation between scales of wind speed, wave height, and sea state

Sea criteria	*Wind speed*			*12-h wind*	*Fully risen sea*			
	Beaufort scale	*Range* ($m\,s^{-1}$)	*Mean* ($m\,s^{-1}$)	*Wave height*[a,b] (m)	*Wave height*[a,b] (m)	*Duration*[b,c] (h)	*Fetch*[b,c] (km)	*Seastate scale*
Mirrorlike	0	< 0.5						0
Ripples	1	0.5–1.7	1.1					1/2
Small wavelets	2	1.8–3.3	2.5	< 0.30	< 0.30			1
Large wavelets, scattered whitecaps	3	3.4–5.4	4.4	0.30–0.61	0.30–0.61	< 2.5	< 19	2
Small waves, frequent whitecaps	4	5.5–8.4	6.9	0.61–1.5	0.61–1.8	2.5–6.5	19–74	3
Moderate waves, many whitecaps	5	8.5–11.1	9.8	1.5–2.4	1.8–3.0	6.5–11	74–185	4
Large waves, whitecaps everywhere, spray	6	11.2–14.1	12.6	2.4–3.7	3.0–5.2	11–18	185–370	5
Heaped-up sea, blown spray, streaks	7	14.2–17.2	15.7	3.7–5.2	5.2–7.9	18–29	370–740	6
Moderately high, longwaves, spindrift	8	17.3–20.8	19.0	5.2–7.3	7.9–11.9	29–42	740–1300	7

From Wenz (1962).
[a]The average height of the highest one-third of the waves (significant wave height).
[b]Estimated from data given in US Hydrographic Office (Washington, DC) publications HO 604 (1951) and HO 603 (1955).
[c]The minimum fetch and duration of the wind needed to generate a fully risen sea.

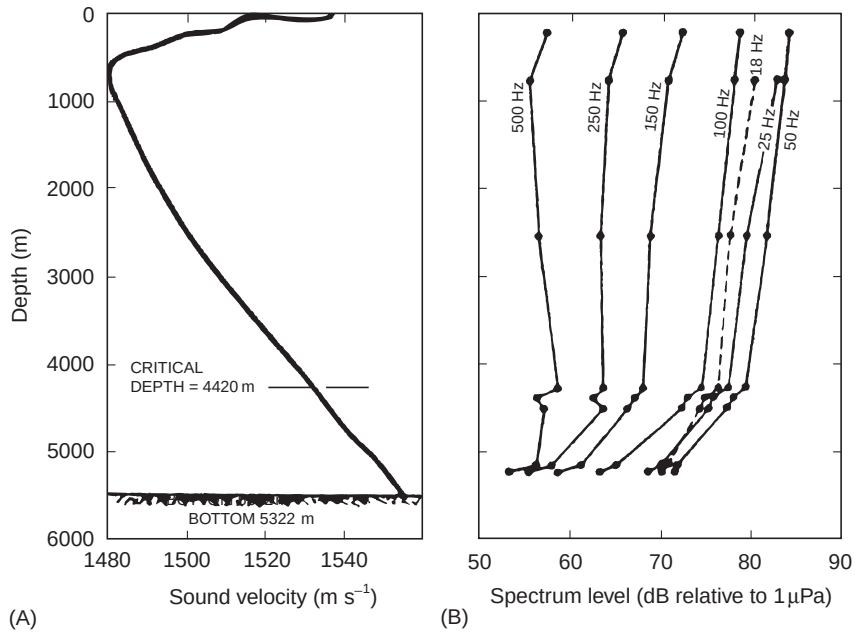

Figure 11 (A) Sound speed profile and (B) noise level as a function of depth in the Pacific. (From Morris (1978).)

equation. The methodology of the sonar equation is analogous to an accounting procedure involving acoustic signal, interference, and system characteristics.

It is instructive, beyond the specific application to conventional sonars, to understand this accounting methodology and below is a simplified summary.

Passive Sonar Equation

A passive sonar system uses the radiated sound from a target to detect and locate the target. A radiating object of source level *SL* (all units are in decibels) is received at a hydrophone of a sonar system at a lower signal level *S* because of the transmission

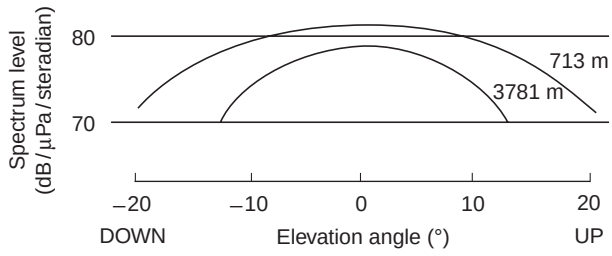

Figure 12 The vertical directionality of noise at the axis of the deep sound channel and at the critical depth in the Pacific. (From Anderson (1979).)

loss '*TL*' it suffers (e.g., cylindrical spreading plus attenuation or a *TL* computed from one of the propagation models) (eqn [14]).

$$S = SL - TL \qquad [14]$$

The noise, *N*, at a single hydrophone is subtracted from eqn [14] to obtain the signal-to-noise ratio (*SNR*) at a single hydrophone (eqn [15]).

$$SNR = SL - TL - N \qquad [15]$$

Typically a sonar system consists of an array or antenna of hydrophones that provides signal-to-noise enhancement through a beamforming process; this process is quantified in decibels by array gain *AG* that is therefore added to the single hydrophone *SNR* to give the *SNR* at the output of the beamformer (eqn [16]).

$$SNR_{BF} = SL - TL - N + AG \qquad [16]$$

Because detection involves additional factors including sonar operator ability, it is necessary to specify a detection threshold (*DT*) level above the SNR_{BF} at which there is a 50% (by convention) probability of detection. The difference between these two quantities is called signal excess (*SE*) (eqn [17]).

$$SE = SL - TL - N + AG - DT \qquad [17]$$

This decibel bookkeeping leads to an important sonar engineering descriptor called the figure of merit, *FOM*, which is the transmission loss that gives a zero signal excess (eqn [18]).

$$FOM = SL - N + AG - DT \qquad [18]$$

The *FOM* encompasses the various parameters a sonar engineer must deal with: expected source level, the noise environment, array gain and the detection threshold. Conversely, since the *FOM* is a transmission loss, one can use the output of a propagation model (or, if appropriate, a simple geometric loss plus attenuation) to estimate the minimum range at which a 50% probability of detection can be expected. This range changes with oceanographic conditions and is often referred to as the 'range of the day' in navy sonar applications.

Active Sonar Equation

A monostatic active sonar transmits a pulse to a target and its echo is detected at a receiver co-located with the transmitter. A bistatic active sonar has the receiver in a different location from the transmitter. The main differences between the passive and active cases is that the source level is replaced by a target strength, *TS*; reverberation and hence reverberation level, *RL*, is usually the dominant source of interference as opposed noise; and the transmission loss is over two paths: transmitter to target and target to receiver. In the monostatic case the transmission loss is $2TL$, where *TL* is the one-way transmission loss; and in the bistatic case the transmission loss is the sum (in dB) over paths from the transmitter to the target and the target to the receiver, $TL_1 + TL_2$. The concept of the detection threshold is useful for both passive and active sonars. Hence, for signal excess, we have eqn [19].

$$SE = SL - TL_1 + TS - TL_2 - (RL + N) + AG - DT \qquad [19]$$

The corresponding *FOM* for an active system is defined for the maximum allowable two-way transmission loss with $TS = 0\,\text{dB}$.

See also

Acoustic Noise. Acoustic Scattering by Marine Organisms. Acoustics, Arctic. Acoustics, Shallow Water. Acoustics in Marine Sediments. Bioacoustics. Bubbles. Deep-sea Drilling Methodology. Seismic Structure. Seismology Sensors. Sonar Systems. Tomography.

Further Reading

Anderson VC (1979) Variations of the vertical directivity of noise with depth in the North Pacific. *Journal of the Acoustical Society of America* 66: 1446–1452.

Brekhovskikh LM and Lysanov YP (1991) *Fundamentals of Ocean Acoustics*. Berlin: Springer-Verlag.

Chapman RP and Harris HH (1962) Surface backscattering strengths measured with explosive sound sources. *Journal of the Acoustical Society of America* 34: 1592–1597.

Chapman RP and Marchall JR (1966) Reverberation from deep scattering layers in the Western North Atlantic. *Journal of the Acoustical Society of America* 40: 405–411.

Collins MD and Siegmann WL (2001) *Parabolic Wave Equations with Applications*. New York: Springer-AIP.

Dushaw BD, Worcester PF, Cornuelle BD and Howe BM (1993) On equations for the speed of sound in seawater. *Journal of the Acoustical Society of America* 93: 255–275.

Jensen FB, Kuperman WA, Porter MB and Schmidt H (1994) *Computational Ocean Acoustics*. Woodbury: AIP Press.

Keller and Papadakis JS (eds) (1977) *Wave Propagation in Underwater Acoustics*. New York: Springer-Verlag.

Makris NC, Chia SC and Fialkowski LT (1999) The biazimuthal scattering distribution of an abyssal hill. *Journal of the Acoustical Society of America* 106: 2491–2512.

Medwin H and Clay CS (1997) *Fundamentals of Acoustical Oceanography*. Boston: Academic Press.

Morris GB (1978) Depth dependence of ambient noise in the Northeastern Pacific Ocean. *Journal of the Acoustical Society of America* 64: 581–590.

Munk W, Worcester P and Wunsch C (1995) *Acoustic Tomography*. Cambridge: Cambridge University Press.

Nicholas M, Ogden PM and Erskine FT (1998) Improved empirical descriptions for acoustic surface backscatter in the ocean. *IEEE-JOE* 23: 81–95.

Northrup J and Colborn JG (1974) Sofar channel axial sound speed and depth in the Atlantic Ocean. *Journal of Geophysical Research* 79: 5633–5641.

Ross D (1976) *Mechanics of Underwater Noise*. New York: Pergamon.

Ogilvy JA (1987) Wave scattering from rough surfaces. *Reports on Progress in Physics* 50: 1553–1608.

Urick RJ (1979) *Sound Propagation in the Sea*. Washington, DC: US GPO.

Urick RJ (1983) *Principles of Underwater Sound*. New York: McGraw Hill.

Spiesberger JL and Metzger K (1991) A new algorithm for sound speed in seawater. *Journal of the Acoustical Society of America* 89: 2677–2688.

Wenz GM (1962) Acoustics ambient noise in the ocean: spectra and sources. *Journal of the Acoustical Society of America* 34: 1936–1956.

ACOUSTICS IN MARINE SEDIMENTS

T. Akal, NATO SACLANT Undersea Research Centre, La Spezia, Italy

Copyright © 2001 Academic Press

doi:10.1006/rwos.2001.0316

Introduction

Because of the ease with which sound can be transmitted in sea water, acoustic techniques have provided a very powerful means for accumulating knowledge of the environment below the ocean surface. Consequently, the fields of underwater acoustics and marine seismology have both used sound (seismo-acoustic) waves for research purposes.

The ocean and its boundaries form a composite medium, which support the propagation of acoustic energy. In the course of this propagation there is often interaction with ocean bottom. As the lower boundary, the ocean bottom is a multilayered structure composed of sediments, where acoustic energy can be reflected from the interface formed by the bottom and subbottom layers or transmitted and absorbed. At low grazing angles, wave guide phenomena become significant and the ocean bottom, covered with sediments of different physical characteristics, becomes effectively part of the wave guide. Depending on the frequency of the acoustic energy, there is a need to know the acoustically relevant physical properties of the sediments from a few centimeters to hundreds of meters below the water/sediment interface.

Underwater acousticians and civil engineers are continuously searching for practical and economical means of determining the physical parameters of the marine sediments for applications in environmental and geological research, engineering, and underwater acoustics. Over the past three decades much effort has been put into this field both theoretically and experimentally, to determine the physical properties of the marine sediments. Experimental and forward/inverse modeling techniques indicate that the acoustic wave field in the water column and seismo-acoustic wave field in the seafloor can be utilized for remote sensing of the physical characteristics of the marine sediments.

Sediment Structure as an Acoustic Medium

Much of the floor of the oceans is covered with a mixture of particles of sediments range in size from boulder, gravels, coarse and fine sand to silt and clay, including materials deposited from chemical and biological products of the ocean, all being saturated with sea water. Marine sediments are generally a combination of several components, most of them coming from the particles eroded from the land and the biological and chemical processes taking place in sea water. Most of the mineral particles found in shallow and deep-water areas, have been transported by runoff, wind, and ice and subsequently distributed by waves and currents.

After these particles have been formed, transported, and transferred, they are deposited to form